

Interactions between Shh, Sostdc1 and Wnt signaling and a new feedback loop for spatial patterning of the teeth

Sung-Won Cho^{1,*}, Sungwook Kwak^{1,*}, Thomas E. Woolley³, Min-Jung Lee¹, Eun-Jung Kim¹, Ruth E. Baker³, Hee-Jin Kim¹, Jeon-Soo Shin², Cheryl Tickle⁵, Philip K. Maini^{3,4} and Han-Sung Jung^{1,†}

SUMMARY

Each vertebrate species displays specific tooth patterns in each quadrant of the jaw: the mouse has one incisor and three molars, which develop at precise locations and at different times. The reason why multiple teeth form in the jaw of vertebrates and the way in which they develop separately from each other have been extensively studied, but the genetic mechanism governing the spatial patterning of teeth still remains to be elucidated. Sonic hedgehog (Shh) is one of the key signaling molecules involved in the spatial patterning of teeth and other ectodermal organs such as hair, vibrissae and feathers. Sostdc1, a secreted inhibitor of the Wnt and Bmp pathways, also regulates the spatial patterning of teeth and hair. Here, by utilizing maternal transfer of 5E1 (an anti-Shh antibody) to mouse embryos through the placenta, we show that Sostdc1 is downstream of Shh signaling and suggest a Wnt-Shh-Sostdc1 negative feedback loop as a pivotal mechanism controlling the spatial patterning of teeth. Furthermore, we propose a new reaction-diffusion model in which Wnt, Shh and Sostdc1 act as the activator, mediator and inhibitor, respectively, and confirm that such interactions can generate the tooth pattern of a wild-type mouse and can explain the various tooth patterns produced experimentally.

KEY WORDS: Shh, Sostdc1, Wnt, Feedback loop, Tooth patterning, Mouse

INTRODUCTION

Ectodermal organs such as teeth, hair, vibrissae and feathers share common morphological features and spatial patterning mechanisms, in which Shh, Wnts and Sostdc1 are key signaling molecules (St-Jacques et al., 1998; Laurikkala et al., 2003; Närhi et al., 2008) but the relationships between these signals are not fully understood. Conditional Shh- and Smo-deficient mice such as *K14-Cre;Shh^{lox/flox}* and *K14-Cre;Smo^{lox/flox}* exhibit the same morphological aberrations in tooth patterns: the first (M1) and second (M2) molars are fused and the dental lamina is absent (Dassule et al., 2000; Gritli-Linde et al., 2002). Interestingly, M1-M2 fusion has also been observed in both *Sostdc1^{-/-}* and *Lrp4^{-/-}* mice, as have a few supernumerary molars and incisors (Kassai et al., 2005; Ohazama et al., 2008). It has been suggested that Sostdc1 is upstream of Shh and that the molar fusion in *K14-Cre;Shh^{lox/flox}*, *K14-Cre;Smo^{lox/flox}*, *Sostdc1^{-/-}* and *Lrp4^{-/-}* mice results from reduction of Shh signals (Ohazama et al., 2008). However, a significant increase in Shh signaling was shown in tooth germs of *Sostdc1^{-/-}* mice, compared with *Sostdc1^{+/-}* mice (Ahn et al., 2010).

Sostdc1 (also known as USAG-1, ectodin and Wise) is an established secreted inhibitor of the Wnt and Bmp pathways (Laurikkala et al., 2003; Yanagita et al., 2004; Kassai et al., 2005; Ohazama et al., 2008; Munne et al., 2009), and Lrp4 is a negative Wnt co-receptor antagonizing the Lrp5- and Lrp6-mediated activation of Wnt signaling (Johnson et al., 2005). The fact that binding of Sostdc1 to Lrp4 inhibits the Wnt pathway could explain the identical tooth phenotype in *Sostdc1^{-/-}* and *Lrp4^{-/-}* mice (Ohazama et al., 2008).

Multiple supernumerary teeth develop in *K14-Cre;Ctnnb1^{(Ex3)fl/+}* and *K14-Cre;APC^{cko/cko}* mice, which show sustained activity of β -catenin in the Wnt pathway in the epithelium (Kuraguchi et al., 2006; Järvinen et al., 2006; Liu et al., 2008). Furthermore, sustained epithelial Wnt/ β -catenin signaling in the hair and teeth of *K14-Cre;Ctnnb1^{(Ex3)fl/+}* mice upregulates *Shh*, *Dkk1* and *Sostdc1*, which suggests that Wnt/ β -catenin signals are upstream of Shh (Närhi et al., 2008; Liu et al., 2008). Furthermore, deletion of *Lef1* or *Wnt10b* severely diminishes the size and the number of fungiform papillae, and decreases expression of *Shh* in tongue fungiform papillae (Iwatsuki et al., 2007). It has also been suggested that epithelial Fgf4, dependent on Wnt signaling, targets *Fgf3* in dental mesenchyme, which, in turn, induces epithelial *Shh* expression together with other mesenchymal signals (Kratochwil et al., 2002). By contrast, it has been shown that Shh suppresses *Wnt10b* in early developing mandibles (Dassule and McMahon, 1998), and that inhibition of Shh signaling by 5E1 (an IgG1 monoclonal antibody against Shh protein) increases the expression of Wnt/ β -catenin signaling in fungiform papillae (Iwatsuki et al., 2007). Furthermore, Wnt signaling in tooth germ of *Sostdc1^{+/-};Shh^{+/-}* mice is significantly elevated compared with that in *Sostdc1^{+/-}* mice (Ahn et al., 2010). All these data taken together suggest that a Wnt-Shh feedback loop involving Sostdc1 and/or other signaling molecules might be involved in patterning the developing teeth.

¹Division in Anatomy and Developmental Biology, Department of Oral Biology, Research Center for Orofacial Hard Tissue Regeneration, Brain Korea 21 Project, Oral Science Research Center, Yonsei University College of Dentistry, Seoul 120-752, Korea. ²Department of Microbiology, Brain Korea 21 Project for Medical Science, Institute for Immunology and Immunological Diseases, and National Core Research Center for Nanomedical Technology, Yonsei University College of Medicine, Seoul 120-752, Korea. ³Centre for Mathematical Biology, Mathematical Institute, University of Oxford, 24-29 St Giles', Oxford OX1 3LB, UK. ⁴Oxford Centre for Integrative Systems Biology, Department of Biochemistry, University of Oxford, South Parks Road, Oxford OX1 3QU, UK. ⁵Department of Biology and Biochemistry, University of Bath, Bath BA2 7AY, UK.

*These authors contributed equally to this work

†Author for correspondence (hsjung@yuhs.ac)

Previously, it was reported that treatment of pregnant tabby mice with an antibody-like recombinant form of EDA1 permanently rescues the Tabby phenotype in offspring (Gaide and Schneider, 2003). Here, by utilizing maternal transfer of 5E1 through the placenta to block Shh signaling (Wang, L. C. et al., 2000), we investigated the changes in tooth patterning and in gene expression to explore whether a Wnt-Shh negative feedback loop mediates tooth patterning and how *Sostdc1* is involved.

Spatial patterning of teeth, characterized by the size and number both of teeth and of their cusps, has been described using a reaction-diffusion mechanism (Jernvall and Thesleff, 2000; Cai et al., 2007), which is based on two main principles (Turing, 1952; Gierer and Meinhardt, 1972; Crampin et al., 2002): (1) the activator promotes its own production and that of an inhibitor, which in turn inhibits activator production; and (2) the inhibitor diffuses faster than the activator. Successful computer models of tooth development already exist (Salazar-Ciudad and Jernvall, 2002; Järvinen et al., 2006; Salazar-Ciudad and Jernvall, 2010). In the most recent mathematical model for tooth patterning, Wnt family genes were suggested as candidates for the activator, and Shh and *Sostdc1* as candidates for inhibitors (Salazar-Ciudad and Jernvall, 2010). However, owing to the high spatial resolution for single teeth produced by these models, they are computationally unable to accommodate splitting and development of multiple structures (Järvinen et al., 2006). Here, we produced a new reaction-diffusion mechanism for spatial patterning of the teeth with the aim of hypothesizing how the sequence of tooth primordia positions could be set by a system of chemicals.

MATERIALS AND METHODS

Drug delivery

A monoclonal antibody (mAb) 5E1 (an IgG1 monoclonal antibody against Shh protein) and a control mAb 40-1a (an IgG1 monoclonal antibody against β -galactosidase) were obtained from hybridoma cells at the Developmental Studies Hybridoma Bank, developed under the auspices of the National Institute of Child Health and Human Development and maintained by the University of Iowa, Department of Biological Sciences (Iowa City, IA, USA). Cyclopamine was purchased from Toronto Research Chemicals (North York, ON, Canada). A single injection of 5E1 (10 mg/kg body weight), 40-1a (10 mg/kg body weight), cyclopamine (10 mg/kg body weight) or PBS (1 ml) was administered intraperitoneally to pregnant ICR mice at embryonic day (E)10, E12, E14 or E16. A double injection of 5E1 or PBS was administered intraperitoneally to pregnant ICR mice at E14 and E17. All newborn mice were allowed to survive for four weeks, after which they were killed for the analysis of tooth and cusp patterns. Alternatively, cultured embryonic tooth germ explants were treated with mAb 5E1 (130 μ g/ml), mAb 40-1a (130 μ g/ml), cyclopamine (10 nM) or PBS (100 μ l/ml) in solution with Dulbecco's Modified Eagle's Medium (DMEM) including 10% foetal bovine serum (FBS). Tooth explants were cultured in vitro for one, two or three days.

Transplantation into kidney

Tooth germs at E12-16 were cultured in medium containing either 5E1 or PBS for two days in vitro and then transplanted into the subcapsular layer of nude mouse kidneys for tooth calcification. All surgical procedures were performed under intraperitoneally administered anaesthesia. No immunosuppressive medication was used. After five weeks the host mice were killed and the kidneys were dissected to obtain the calcified teeth.

Three-dimensional reconstructions

For three-dimensional reconstructions, images of frontal serial sections of the developing molars stained with Haematoxylin and Eosin were imported into the 'Reconstruct' software developed by J. C. Fiala and K. M. Harris at Boston University (MA, USA). Images were aligned manually and the shape of the epithelium was traced manually along the basement membrane. Every third image was employed in the reconstruction and the

actual reconstructed thickness was 21 μ m. Three-dimensional reconstructed computed tomography images were obtained by scanning the calcified teeth using micro-computed tomography (Micro-CT, Skyscan 1076, Skyscan, Antwerp, Belgium). The data were then digitalized using a frame grabber and the resulting images were transmitted to a computer with topographic reconstruction software.

Microarray analysis

Gene-chip expression analysis was performed with RNA from mandibular tooth germs from embryos of pregnant mice at one day after injection (PBS, $n=2$; 40-1a, $n=2$; cyclopamine, $n=2$; 5E1, $n=2$), using a mouse gene microarray (GeneChip Mouse Genome 430 2.0, Affymetrix, Santa Clara, CA, USA). A gene-chip scanner (GeneChip Scanner 3000, Affymetrix) was used to measure the intensity of the fluorescence emitted by the labeled target. Raw image data were converted to cell-intensity (CEL) files using the Affymetrix GeneChip Operating System, and these CEL files were normalized using the MARS 5.0 algorithm. Following statistical analysis, differentially expressed genes were selected using GenePlex software version 3.0 (ISTECH, Seoul, Korea). Differentially expressed genes with changes of at least 1.5-fold in the 5E1-treated group compared with the control group were selected, and then analyzed statistically using Student's *t*-test with the level of statistical significance set at $P<0.01$. Microarray data have been deposited in GEO with accession number GSE27429.

Quantitative reverse-transcriptase polymerase chain reaction (RT-qPCR) analysis

RNA was extracted from mandibular tooth germs from embryos at one day after injection (PBS, $n=2$; 40-1a, $n=2$; cyclopamine, $n=2$; 5E1, $n=2$). RT-qPCR was performed using a Thermal Cycler Dice Real-Time System and SYBR Premix EX Taq (Takara, Japan) according to the manufacturer's instructions. For RT-qPCR, the reaction mixture was initially incubated for one minute at 95°C. The amplification program comprised 40 cycles of denaturation at 95°C for 5 seconds, annealing at 55-60°C for 10 seconds, and extension at 72°C for 10 seconds. The RT-qPCR for each sample was performed in triplicate and the amount of each of the RT-qPCR products was normalized using β -2-microglobulin as an internal control. The data were analyzed with the Thermal Cycler Dice Real-Time System analysis software and the $2^{-\Delta\Delta C_t}$ method. The statistical calculations were performed using *t*-test of variables to determine significant changes at the 95% confidence level ($P<0.05$).

Protein-bead implantation

Affi-Gel blue beads (Bio-Rad Laboratories, Hercules, CA, USA) were soaked with the Shh recombinant protein (1 μ g/ μ l; mouse Shh-N, R&D Systems, Minneapolis, MN, USA). Control beads were prepared similarly by soaking them in PBS at room temperature for at least 1 hour. The mandibular M1 tooth germs of wild-type mice at E14 were dissected and incubated in Dispase II (Roche, Mannheim, Germany) at 1.2 U/ml in PBS for 20 minutes, and the dental epithelium and mesenchyme were separated. Beads were placed on dental epithelium, mesenchyme or the lingual side of intact tooth germs, which was then cultured for 1 day in DMEM including 10% FBS. Whole-mount in-situ hybridization was then carried out.

In situ hybridization

Tissues were fixed overnight in 4% paraformaldehyde. Hybridizations were performed on these tooth germs with digoxigenin-labeled cRNA probes in hybridization buffer for 18 hours at 72°C. Hybridization signals were detected by alkaline-phosphatase-conjugated anti-digoxigenin antibodies plus nitro blue tetrazolium chloride and 5-bromo-4-chloro-3-indolyl phosphate, toluidine salt substrate (Roche, Mannheim, Germany).

Mathematical simulation

In order to model spatial pattern formation for teeth in wild-type mice, a system of reaction-diffusion equations, modified from the Gierer-Meinhardt system (Gierer and Meinhardt 1972) to allow the inclusion of a mediator species, was simulated. The equations simulated are

$$\begin{aligned}\partial A/\partial t &= D_a \nabla^2 A + A/I - \beta A + \alpha, \\ \partial M/\partial t &= D_m \nabla^2 M + \mu (A^2 - M), \\ \partial I/\partial t &= D_i \nabla^2 I + \delta (M - AI),\end{aligned}$$

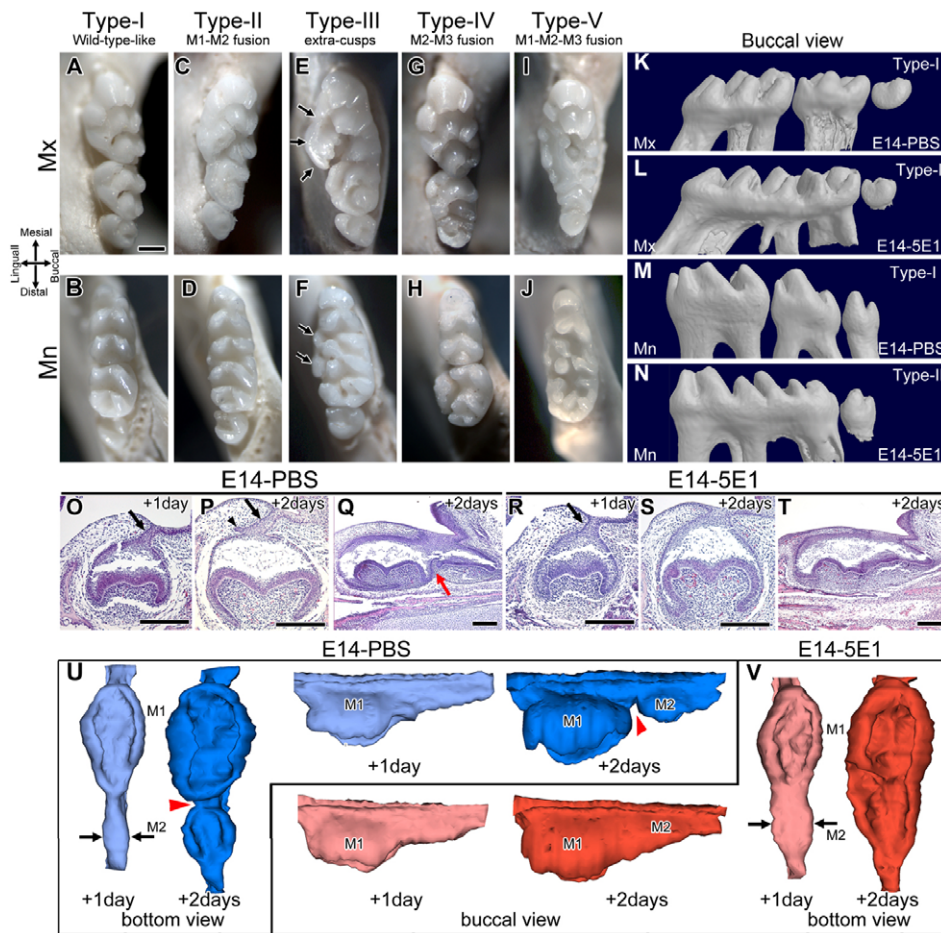


Fig. 1. Morphological changes in molar spatial patterning in mouse after maternal transfer of 5E1. (A–J) Five types of molar patterns obtained in maxilla (Mx) and mandible (Mn): Type-I, wild-type-like with first (M1), second (M2) and third (M3) molar; Type-II, M1-M2 fusion; Type-III, M1-M2 fusion with extra lingual cusps (arrows); Type-IV, M2-M3 fusion; Type-V, M1-M2-M3 fusion. (K–N) Three-dimensional micro-computed-tomography images showing buccal aspect of type-I and type-II patterns at embryonic day (E) 14 after injection of phosphate-buffered saline (E14-PBS) and after 5E1 injection (E14-5E1) in maxilla and mandible. (O–T) Dental lamina (arrow) is evident in the frontal section of M1 in both E14-PBS and E14-5E1 at one day after injection (O,R). After two days, dental lamina and lingual epithelial bud (arrowhead) are observed only in an E14-PBS (compare P with S), and M1-M2 separation (red arrow) is evident in E14-PBS (Q). M1-M2 fusion is evident in E14-5E1 (T). (U,V) Three-dimensional images of dental epithelium from bottom view show the larger buccolingual diameter of M2 (between arrows) in E14-5E1 (V) than in E14-PBS (U) after one day. The boundary (red arrowheads) between M1 and M2 is clearly shown in E14-PBS after two days both from bottom and buccal view (U), whereas M1-M2 fusion is evident in E14-5E1 (V). Scale bars: 500 μ m.

where A , M and I are activator, mediator and inhibitor concentration, respectively. The rectangular domain grows apically in the x -direction. The length (l) of the domain is governed by $l(t) = 3\gamma(t)$, where $\gamma(t) = 1 + 5t/(t + 500)$.

The initial domain was $\Omega = [0, 3] \times [0, 3]$ with pseudo-random initial conditions (for details, see Crampin et al., 2002). The activator and inhibitor are simulated with Dirichlet (fixed) boundary conditions ($A = I = 0$ on $\partial\Omega$) and the mediator is simulated with Neumann (zero flux) boundary conditions ($\partial M/\partial n = 0$ on $\partial\Omega$ where n is the outward facing normal vector on the boundary, which means that no mediator leaves through the domain boundary). In order to attain the decreasing spatial scale of tooth germs, a spatially varying gradient of one of the parameters of the form $\mu \rightarrow \mu \exp(x\gamma(t)/32)$ was applied. The growth function allows the domain to grow quickly initially and then slow down until the domain attains a finite definite length, in this case a non-dimensional length of 18. Parameters are $D_a = 0.1$, $D_m = 0.9$, $D_i = 0.1$, $\alpha = 0.1$, $\beta = 0.5$, $\mu = 0.4$, $\delta = 100$.

RESULTS

Molar fusion and supernumerary tooth formation are induced by blocking Shh activity in vivo

Mice delivered from pregnant mice injected with 5E1 between E10 and E18 exhibited normal or abnormal spatial patterns of molars, and reduced body and skull size (Fig. 1; Table 1), whereas all mice delivered from pregnant mice injected with cyclopamine (a specific Smo antagonist), phosphate-buffered saline (PBS) or a control antibody of 40-1a (an IgG1 monoclonal antibody against β -galactosidase), were normal in molar patterning and body size. No changes were detected in the injected pregnant mice. The molar patterns observed in both the maxilla and the mandible following embryonic exposure to 5E1

can be divided into the following five types: type-I, wild-type-like (having three molars); type-II, M1-M2 fusion; type-III, M1-M2 fusion with extra lingual cusps; type-IV, M2-third molar (M3) fusion; type-V, M1-M2-M3 fusion (type-I-V in Fig. 1A–N). All tooth germs are at the primary epithelial band stage at E10. Whereas M1 is at the dental lamina stage, cap stage and bell stage at E12, E14 and E16, respectively, M2 is at the dental lamina stage, cap stage and bell stage at E14, E16 and E18, respectively. A number of mice that were exposed to 5E1 at E10 (E10-5E1) or E12 (E12-5E1) exhibited M1-M2 fusion in the maxillary and/or mandibular quadrants, but M1-M2 fusion was most frequent in 5E1-exposed mice at E14 (E14-5E1) (48/78 in the maxilla and 53/82 in the mandible; Table 1, Fig. 1C–F, K–N; Fig. 2H–K). Mice exposed to 5E1 at E16 (E16-5E1) exhibited no M1-M2 fusion but did exhibit M2-M3 fusion, which was evident in both the maxilla and mandible (Fig. 1G, H). Mice exposed to 5E1 at E18 (E18-5E1) exhibited no fused molars. These findings demonstrate that the pivotal developmental times to enhance M1-M2 fusion and M2-M3 fusion are from E14 to E15 and from E16 to E17, respectively. The finding that 5E1 injection could not induce the M1-M2 fusion at E16 and the M2-M3 fusion at E18 indicates that molars at the bell stage have been already separated from other tooth germs. When 5E1 was injected twice into pregnant mice so that embryos would be exposed at stage E14 and then at stage E17, M1-M2-M3 fusion occurred in both the maxilla and mandible (Fig. 1I, J). In addition, extra incisors or molars, which have been reported in *Sostdc1*^{-/-} and *Lrp4*^{-/-} mice, were found in E12-5E1, E14-5E1 and E16-5E1 mice, but not in the PBS-treated E14 mice (E14-PBS) (Fig. 2A–E).

In order to investigate how these tooth fusions arise following 5E1 treatment, sections were taken through the developing teeth of embryos at two days after 5E1 injection at E14. Frontal sections showed that the lingual epithelial bud, which is known to be a rudiment of a secondary tooth (Khaejornbut et al., 1991), and dental lamina were present in E14-PBS (Fig. 1P) but absent in E14-5E1 after two days (Fig. 1S). This result is consistent with findings in *K14-Cre;Shh^{fllox/fllox}* and *K14-Cre;Smo^{fllox/fllox}* mice. Secondly, M1-M2 fusion was evident in sagittal sections of the mandible in E14-5E1 at two days after injection, whereas M1 was separated from M2 in E14-PBS (Fig. 1Q,T). In E14-PBS, after two days M2 could be seen to be clearly separated from M1 in three-dimensional reconstructed images of dental epithelium (red arrowheads in Fig. 1U), whereas the boundary between M1 and M2 was not clear in E14-5E1 (Fig. 1V). Moreover, the buccolingual diameter of M2 was larger in E14-5E1 than in E14-PBS after one day, which suggests that M2 development was accelerated by 5E1 treatment (Fig. 1U,V).

It should be noted that transparent enamel can be seen to cover the dentine in sagittal sections of fused molars in E14-5E1 mice (Fig. 2F,G), in contrast to the enamel defects reported in *K14-Cre;Shh^{fllox/fllox}* and *K14-Cre;Smo^{fllox/fllox}* mice. Enamel formation occurring postnatally might not be affected by a single 5E1 injection at E14.

Molar fusion is also induced by blocking of Shh activity in vitro

A parallel series of experiments was carried out in which tooth germs at E14 were cultured for two days in a medium containing 5E1, cyclopamine, 40-1a and PBS, and then grafted under kidney capsules for five weeks to undergo calcification. In contrast to the in vivo results, M1-M2 fusion was induced by cyclopamine as well as 5E1 after two days of culture in vitro (see Fig. S1 in the supplementary material). This discrepancy is attributable to the fact that cyclopamine is no longer active in vivo a few hours after intraperitoneal injection (Lipinski et al., 2008) but is active in culture medium for two days. Consistent with in vivo 5E1 results, M1-M2 fusion was evident in the E14-5E1 calcified teeth developing in the kidney for five weeks, and M2-M3 fusion was evident in the E16-5E1 teeth (see Fig. S1 in the supplementary material), demonstrating again that the pivotal stages for producing M1-M2 fusion and M2-M3 fusion are E14 and E16, respectively.

Shh activity is effectively blocked by maternal transfer of 5E1

Many signaling pathways (e.g. those involving Bmp, Fgf, Wnt, Tnf and Shh) are involved in tooth development (Jernvall and Thesleff, 2000), and the enamel knot, a signaling center in dental epithelium, expresses many signaling molecules such as *Bmp2*, *Bmp4*, *Bmp7*, *Fgf3*, *Fgf4*, *Fgf9*, *Fgf20*, *Wnt10a*, *Wnt10b* and *Shh* (Thesleff, 2003). In order to ascertain whether Shh signaling in developing teeth is blocked by maternal transfer of 5E1, we investigated the transcriptional profiles of tooth germs 24 hours after injection at E14 focusing on genes known to be regulated by Shh signaling. In the microarray analysis, *Gli1* and *Ptch1*, direct targets of hedgehog signaling (Wang, B. et al., 2000), were downregulated in E14-5E1 tooth germs more than fourfold compared with E14-40-1a, E14-PBS and E14-cyclopamine (Table 2), and *Ptch1* and *Gli1* were downregulated in E14-5E1 tooth germs compared with E14-PBS in the RT-qPCR analysis (Fig. 3). Furthermore, *Hhip*, another target of hedgehog, was also downregulated in E14-5E1 more than twofold compared with E14-40-1a and E14-PBS in microarray (see Table S1 in the supplementary material), and RT-qPCR confirmed this

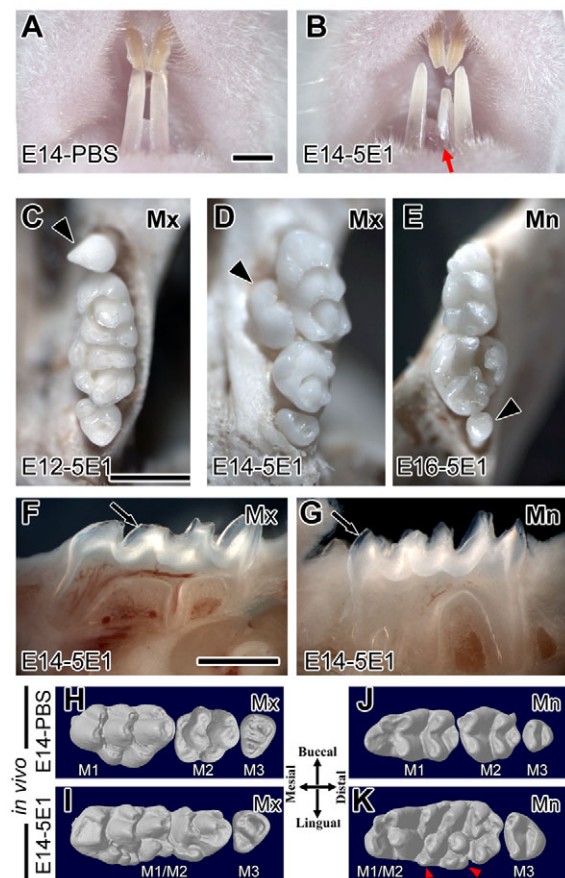


Fig. 2. Morphological changes in mouse molars after 5E1 treatment in vivo. (A,B) Supernumerary incisors (red arrow) develop in embryonic day (E) 14 mice treated with 5E1 (B, E14-5E1; 2/82 in mandibular quadrants) but not in control mice treated with PBS (A, E14-PBS). (C-E) Supernumerary molars (arrowheads) develop in E12-5E1 [1/40 in the maxillary quadrants (C), 1/32 in the mandibular quadrants], E14-5E1 (4/78 in the maxillary quadrants, D) and E16-5E1 (1/54 in the mandibular quadrants, E). (F,G) Transparent enamel (arrows) is seen covering the dentine in sagittal sections of fused molars in Mx and Mn of E14-5E1. (H-K) Three-dimensional images from occlusal view show pattern of molars in 4-week-old E14-PBS and E14-5E1. E14-PBS mice have three molars in Mx (H) and Mn (J). M1-M2 fusion is observed in Mx (I) and Mn (K) of E14-5E1. Extra cusps are evident on lingual side of a fused molar (red arrowheads in K). Scale bars: 1 mm; Mx, maxilla; Mn, mandible.

downregulation of *Hhip* in E14-5E1 (Fig. 3). Conversely, expression of *Smo*, *Gli2* and *Gli3*, which are not activated in response to Shh signaling but are involved in Shh signal transcription (Wang, B. et al., 2000), was not changed by 5E1 in the microarray and RT-qPCR analyses (see Table S1 and Fig. S2 in the supplementary material). *Shh* expression level in the microarrays was not significantly changed but appeared to be increased at least 1.4-fold after 5E1 treatment (see Table S1 in the supplementary material).

These results suggest that 5E1 blocked Shh activity in developing teeth significantly and selectively, by binding not with *Shh* mRNA but with Shh protein. In addition, *Ptch1* expression disappeared in the dental epithelium and mesenchyme following treatment with 5E1 (compare Fig. 4F,H with 4E,G; see Fig. S3 in the supplementary material). In contrast to the *Ptch1* expression, the *Shh* expression pattern was the same in E14-PBS and E14-5E1 mice in vivo at one day after 5E1 injection (Fig. 4A,B; see Fig. S3 in the supplementary

Table 1. Various spatial patterns of molars in mice after being exposed to 5E1

Stage	Injection	Molar patterns in maxillary quadrant					Molar patterns in mandibular quadrant						
		Total number	Type-I (%)	Type-II (%)	Type-III (%)	Type-IV (%)	Type-V (%)	Total Number	Type-I (%)	Type-II (%)	Type-III (%)	Type-IV (%)	Type-V (%)
E10	PBS	56	100	0	0	0	0	56	100	0	0	0	0
	40-1a	54	100	0	0	0	0	54	100	0	0	0	0
	Cyclopamine	44	100	0	0	0	0	44	100	0	0	0	0
E12	5 E1	32	53.1	46.9	0	0	0	30	100	0	0	0	0
	PBS	52	100	0	0	0	0	52	100	0	0	0	0
	40-1a	40	100	0	0	0	0	40	100	0	0	0	0
E14	Cyclopamine	40	100	0	0	0	0	40	100	0	0	0	0
	5 E1	40	65	35	0	0	0	32	81.25	0	18.75	0	0
	PBS	52	100	0	0	0	0	52	100	0	0	0	0
E16	40-1a	44	100	0	0	0	0	44	100	0	0	0	0
	Cyclopamine	38	100	0	0	0	0	38	100	0	0	0	0
	5 E1	78	38.5	30.75	30.75	0	0	82	35.4	25.6	39.0	0	0
E18	PBS	26	100	0	0	0	0	26	100	0	0	0	0
	5 E1	54	85.2	0	0	14.8	0	54	44.4	0	0	55.6	0
E14 and E17	PBS	28	100	0	0	0	0	28	100	0	0	0	0
	5 E1	40	100	0	0	0	0	40	100	0	0	0	0
E14 and E17	5 E1	26	30.8	23.1	38.4	0	7.7	26	30.8	15.4	38.4	0	15.4

material). *Shh* expression in M2 appeared in E14-5E1 mice in vitro whereas it was not present in E14-PBS specimens (Fig. 4C,D). This change might be attributable to the accelerated development of M2 after 5E1 injection. Taken together, all these results indicate that 5E1 significantly blocked Shh activity in developing teeth within 24 hours and also suggest that *Shh* expression in M2 might be elevated and/or accelerated by 5E1 treatment in vitro.

Sostdc1 is regulated by Shh during tooth development

Microarray and RT-qPCR analyses showed that blocking Shh signaling via 5E1 treatment downregulated *Sostdc1* expression levels more than twofold (Fig. 3, Table 2). E14-PBS mice exhibited *Sostdc1* expression in the dental epithelium and mesenchyme in vivo and in vitro (Fig. 4I,K; see Fig. S3 in the supplementary material), but *Sostdc1* was weakly expressed in dental epithelium and absent in dental mesenchyme of E14-5E1 (Fig. 4J,L; see Fig.

S3 in the supplementary material). Furthermore, exogenous Shh protein induced *Sostdc1* expression in dental mesenchyme of wild-type mice at E14 (Fig. 5H) but not in dental epithelium (Fig. 5F). By contrast, ectopic *Ptch1* expression was clearly induced around the Shh bead in both the epithelium and mesenchyme, indicating good efficiency of exogenously applied Shh protein (Fig. 5B,D). Interestingly, *Ptch1* was widely expressed both in the PBS- and Shh-treated dental epithelium after one day in culture (Fig. 5A,B). *Sostdc1* was not induced around either PBS or Shh beads which were placed on the wild-type tooth germs at E14 without separation of epithelium and mesenchyme (Fig. 5I-L).

Wnt and Fgf signaling in epithelium are upregulated after blocking of Shh activity

Expression levels of β -catenin and *Lef1* were not changed after blocking Shh activity by 5E1 treatment at E14 according to the microarray analysis, and *Lef1* expression pattern was not detectably

Table 2. Genes with at least twofold difference in expression as determined by microarray analysis after 5E1 injection compared with after 40-1a, PBS or cyclopamine injection*

Gene symbol	Gene name	Reference sequence	Fold change		
			5E1 versus 40-1a	5E1 versus cyclopamine	5E1 versus PBS
Upregulated genes					
<i>Fgf20</i>	fibroblast growth factor 20	NM_030610	2.30	2.49	2.75
<i>Krt73</i>	keratin 73	NM_212485	2.67	2.92	3.42
Downregulated genes					
<i>Aldh1a3</i>	aldehyde dehydrogenase family 1, subfamily A3	NM_053080	-2.02	-2.36	-2.70
<i>Ambn</i>	ameloblastin	NM_009664	-2.16	-2.71	-3.12
<i>Cbln1</i>	cerebellin 1 precursor protein (similar to precerebellin-1)	NM_019626	-2.13	-2.46	-3.03
<i>Foxf2</i>	forkhead box F2	NM_010225	-2.31	-2.49	-3.64
<i>Gli1</i>	GLI-Kruppel family member GLI1	NM_010296	-4.81	-5.68	-5.30
<i>Kcnj8</i>	potassium inwardly-rectifying channel, subfamily J, member 8	NM_008428	-2.59	-3.15	-3.77
<i>Krt36</i>	keratin 36	NM_008472	-3.03	-3.86	-2.39
<i>Ntrk2</i>	neurotrophic tyrosine kinase, receptor, type 2	NM_001025074	-2.90	-3.12	-3.12
<i>Ptch1</i>	patched homolog 1	NM_008957	-4.82	-4.15	-5.15
<i>Slco4a1</i>	solute carrier organic anion transporter family, member 4a1	NM_148933	-3.29	-3.65	-3.12
<i>Sostdc1</i>	sclerostin domain containing 1	NM_025312	-2.62	-2.59	-3.02
<i>Syt16</i>	synaptotagmin XVI	NM_172804	-2.74	-2.93	-3.02

*Student's *t*-test was employed for statistical analysis with level of statistical significance set at $P < 0.01$.

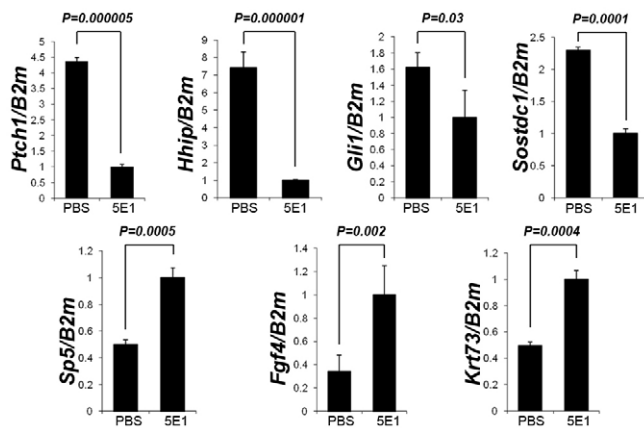


Fig. 3. Transcriptional changes in molars after maternal transfer of 5E1 into mouse embryos at E14. RT-qPCR analysis shows up- or downregulation of *Ptch1*, *Hhip*, *Gli1*, *Sostdc1*, *Sp5*, *Fgf4* and *Krt73*. The amount of each of the RT-qPCR products was normalized using β -2-microglobulin (*B2m*) as an internal control. Student's *t*-test was performed for statistical analysis with level of statistical significance set at $P < 0.05$. Error bars indicate s.d. on the normalized ratio.

changed as judged by in situ hybridization after in vitro culture (Fig. 4S,T). Nevertheless, Wnt signaling seems to be upregulated as judged by expression of *Sp5*, which was increased in the microarray and RT-qPCR analyses (Fig. 3; see Table S1 in the supplementary material). *Sp5* is a direct transcriptional target of the Wnt/ β -catenin pathway, and the promoter region of *Sp5* contains multiple binding sites for Lef1 and Tcf family members (Weidinger et al., 2005; Zhang et al., 2008). In addition, *krt73*, which is regulated by *Sp5* in hair (Zhang et al., 2008), was increased in the microarray and RT-qPCR analyses following 5E1 treatment (Fig. 3, Table 2) and also seen to be expressed more widely by in situ hybridization after culture in vitro (Fig. 4U,V). *Sp5* is expressed in dental epithelium of developing M1 at E12 and E14, and its expression is observed mainly in the epithelium of M2 at E16 (see Fig. S4 in the supplementary material). In our experiment, *Sp5*-expressing areas in M1 and M2 were separated in E14-PBS, but connected in E14-5E1 (Fig. 4M-P).

Although mesenchymal Fgf genes such as *Fgf3* and *Fgf10* did not display any significant change in gene expression levels, epithelial Fgf genes exhibited significant changes after 5E1 treatment. *Fgf9* and *Fgf20*, expressed in enamel knot, showed significantly increased expression levels in E14-5E1 (Table 2; see Table S1 in the supplementary material) in the microarray analysis, and *Fgf4* expression was increased in the RT-qPCR analysis (Fig. 3). An *Fgf4*-expressing enamel knot appeared in M2 after one day in vitro in E14-5E1 tooth germs but not in E14-PBS (Fig. 4W,X), which indicates accelerated M2 development.

Sostdc1 has also been implicated as a Bmp antagonist. *Bmp4* expression was downregulated >1.5-fold after 5E1 treatment in the microarray and RT-qPCR analyses (see Table S1 and Fig. S2 in the supplementary material), but other signals in the Bmp pathway such as *Bmp2*, *Bmp5*, *Bmp7*, *Bmpr1a*, *Msx1* and *Msx2* exhibited minor changes in expression level after 5E1 treatment in the microarray analysis (see Table S1 in the supplementary material). Expression levels of other known Bmp antagonists such as *Grem1* and *Nog* were not changed in either the microarray or RT-qPCR analyses (see Table S1 and Fig. S2 in the supplementary material).

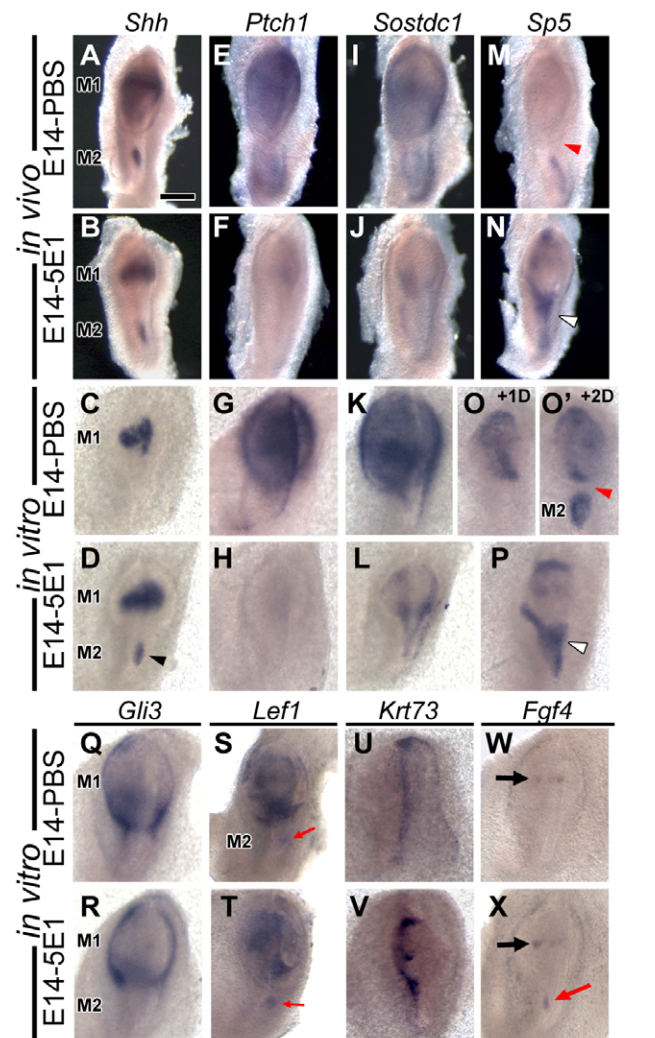


Fig. 4. Alterations in gene expression pattern in 5E1-treated mouse molars. (A-D) Whereas the pattern of *Shh* expression is the same in E14-PBS and E14-5E1 mice after one day in vivo (A,B), *Shh* expression in M2 (black arrowhead) is evident only in E14-5E1 in vitro, showing accelerated M2 development (compare D with C). (E-H) *Ptch1* is strongly expressed in E14-PBS in vivo (E) and in vitro (G), but disappeared in E14-5E1 (F,H). (I-L) *Sostdc1*-expressing areas are markedly reduced in E14-5E1 (J,L) compared with E14-PBS (I,K). (M-P) *Sp5* expression in M1 and M2 is separated in E14-PBS in vivo (red arrowhead in M). *Sp5* is observed in M1 of E14-PBS after one day (+1D) culture in vitro (O) and expressed in M1 and M2 separately after two days (+2D) (red arrowhead in O'), but connected in E14-5E1 in vivo and from one day in culture (white arrowheads in N and P). (Q,R) *Gli3* expression pattern of E14-PBS is the same as that of E14-5E1 after one day in vitro. (S,T) *Lef1* expression is observed in M1 after one day in vitro in both E14-PBS and E14-5E1, but its domain of expression in M2 (red arrows) is larger in E14-5E1 (T) than in E14-PBS (S). (U,V) *krt73* is expressed in a line in E14-PBS (U), but is widely expressed throughout M1 and M2 in E14-5E1 (V). (W,X) *Fgf4* expression in M1 (black arrow) is evident in both E14-PBS (W) and E14-5E1 (X), but its expression in M2 (red arrow) is only present in E14-5E1 (X). Scale bar: 200 μ m

M2 development is accelerated by blocking of Shh activity

The buccolingual diameter of M2 was larger in E14-5E1 than in E14-PBS after one day in vivo (Fig. 1U,V), and *Shh*, *Sp5* and *Fgf4* expression in M2 appeared in E14-5E1 but not in E14-PBS after

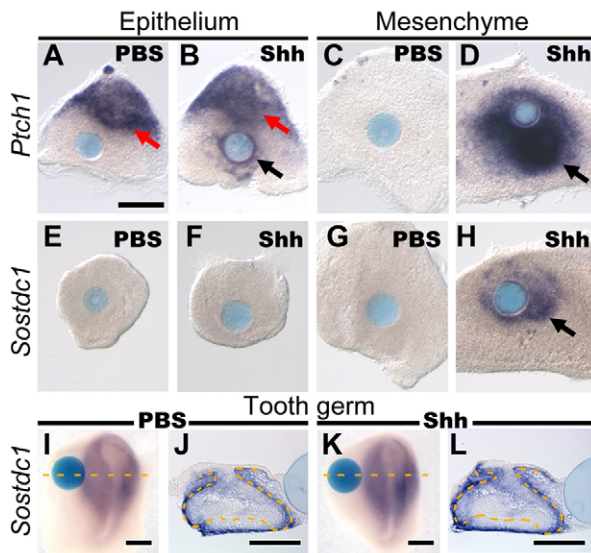


Fig. 5. Effects of Shh on *Sostdc1* expression in mouse. (A–D) Apart from endogenous *Ptch1* (red arrows in A and B), exogenous *Ptch1* is expressed around the Shh protein bead in both dental epithelium and mesenchyme (black arrows in B,D), but not around PBS beads (A,C). (E–H) *Sostdc1* is not expressed around the control PBS beads (E,G). *Sostdc1* is induced by exogenous Shh protein in mesenchyme (arrow in H), but not in epithelium (F). (I–L) *Sostdc1* is expressed in dental epithelium and mesenchyme around wild-type tooth germs at E14 but is not induced in either epithelium or mesenchyme around beads soaked in Shh protein. Occlusal views are shown in I and K. Frontal section is shown in J and L at the level of the dashed lines in I and K, respectively. Yellow dashed lines indicate the boundary of the dental epithelium and mesenchyme. Scale bars: 200 μm .

one day culture in vitro (Fig. 4C,D,O,P,W,X). Furthermore, *Leffl* expression in M2 (red arrow) is larger in E14-5E1 than in E14-PBS after one day in vitro (Fig. 4S,T). These results indicate that M2 development was accelerated by 5E1 treatment.

This accelerated M2 development might be attributable to the downregulation of mesenchymal *Sostdc1* that resulted from blocking Shh activity, as the inhibitory role of mesenchymal *Sostdc1* has been suggested by previous studies, in which development of M2 was promoted when M2 was separated from M1 at E14 (Kavanagh et al., 2007) and additional incisors were formed when the dental mesenchyme of a developing incisor is removed (Munne et al., 2009). Our results are thus consistent with the role of mesenchymal *Sostdc1* in inhibiting the development of subsequent tooth germs.

A new reaction-diffusion model for spatial patterning of teeth

In tooth development, *Leffl* is expressed in the enamel knot and its neighboring mesenchyme (Kratochwil et al., 2002), whereas *Sostdc1* expression (Laurikkala et al., 2003) is observed mainly outside the *Leffl*-expressing area (Fig. 6A,B). These expression patterns can be modeled by a reaction-diffusion mechanism. Wnt signals in the enamel knot induce *Shh* expression in the enamel knot through the induction of *Fgf4* and *Fgf3* (Kratochwil et al., 2002; Liu et al., 2008), and then both Wnt and Shh proteins diffuse laterally. Wnt signaling induces *Leffl* in the enamel knot and its neighboring mesenchyme (Kratochwil et al., 2002), whereas Shh has long-range activity and induces broad

expression of Shh signaling target genes in the dental epithelium and mesenchyme (Gritli-Linde et al., 2001). *Sostdc1* expression regulated by Shh signaling in our study is found mainly outside the *Leffl*-expressing area and produces the secreted *Sostdc1* that also diffuses to antagonize Wnt/ β -catenin signals (Fig. 6C). Additionally, the reason why *Sostdc1* is not induced by Shh in the *Leffl*-expressing area might be that Wnt preoccupies this area and inhibits *Sostdc1*. These interactions between Wnt, Shh and *Sostdc1* lead us to propose a Wnt-Shh-*Sostdc1* negative feedback loop and a new reaction-diffusion model consisting of activator, mediator and inhibitor which are Wnt, Shh and *Sostdc1*, respectively (Fig. 6E). The key principles in this model are: (1) an activator promotes its own production and that of a mediator, (2) the mediator diffuses faster than the activator, and (3) inhibitor production is induced by the mediator but suppressed by the activator.

This new model for spatial patterning of the teeth can account for various molar patterns (Fig. 6D). Each tooth in wild-type mice has both the *Leffl*-expressing activation zone and the *Sostdc1*-expressing inhibition zone resulting from the Wnt-Shh-*Sostdc1* loop, which separates M1, M2 and M3 from each other. In our experiments, 5E1 blocks interactions between mediator and inhibitor by blocking Shh proteins, which induces loss of the inhibition zone and then fusion of molars. The deficiency in the mediator results in fused molars in *K14-Cre;Shh^{fllox/fllox}* and *K14-Cre;Smo^{fllox/fllox}* mice, whereas molar fusion in *Sostdc1^{-/-}* and *Lrp4^{-/-}* mice is attributable to the absence of the inhibitor and its receptor, respectively, as *Lrp4*-*Sostdc1* binding is necessary to inhibit the Wnt pathway (Ohazama et al., 2008). Multiple supernumerary teeth develop in *K14-Cre;Ctnnb1^{(Ex3)fl/-}* and *K14-Cre;APC^{cko/cko}* mice (Kuraguchi et al., 2006; Järvinen et al., 2006) as a result of multiple activation and inhibition zones originating from multiple Wnt/ β -catenin signals, which act as the activator in the Wnt-Shh-*Sostdc1* loop. Furthermore, we verified, by using the new reaction-diffusion model consisting of activator, mediator and inhibitor, that such interactions do indeed lead to tooth patterning consistent with that of wild-type mice (Fig. 6F; see Movie 1 in the supplementary material).

DISCUSSION

Tooth patterns of 5E1-treated mice are similar to those seen in transgenic mice with Shh signaling defects

Here, we have used a simple system in which 5E1, a Shh antibody, is injected into pregnant mice at precise times to investigate Shh signaling in patterning of the teeth in embryos. Analysis of expression of *Ptch1* and *Gli1*, known gene targets of Shh signaling, indicated that 5E1 injection blocked Shh activity in developing teeth. The binding efficiency of 5E1 to Shh, Ihh and Dhh proteins has been evaluated in a previous study and it was found that 5E1 (10 $\mu\text{g/ml}$) completely blocked Shh (2 $\mu\text{g/ml}$)-induced differentiation of C3H10T1/2 cells (Wang, L. C. et al., 2000). *Ihh* and *Dhh* are not expressed in developing teeth so in our experiments only Shh activity will be blocked. We found, using our treatment regime, that we could replicate various tooth patterns previously observed in *K14-Cre;Shh^{fllox/fllox}* and *K14-Cre;Smo^{fllox/fllox}* transgenic mice including M1-M2 fusion and M1-M2-M3 fusion (Dassule et al., 2000; Gritli-Linde et al., 2002). Interestingly M2-M3 fusions produced in our study have never been reported before, probably because we can manipulate the time at which Shh signaling is blocked. In addition, our study, like the previous studies in *K14-Cre;Shh^{fllox/fllox}* and *K14-Cre;Smo^{fllox/fllox}* mice

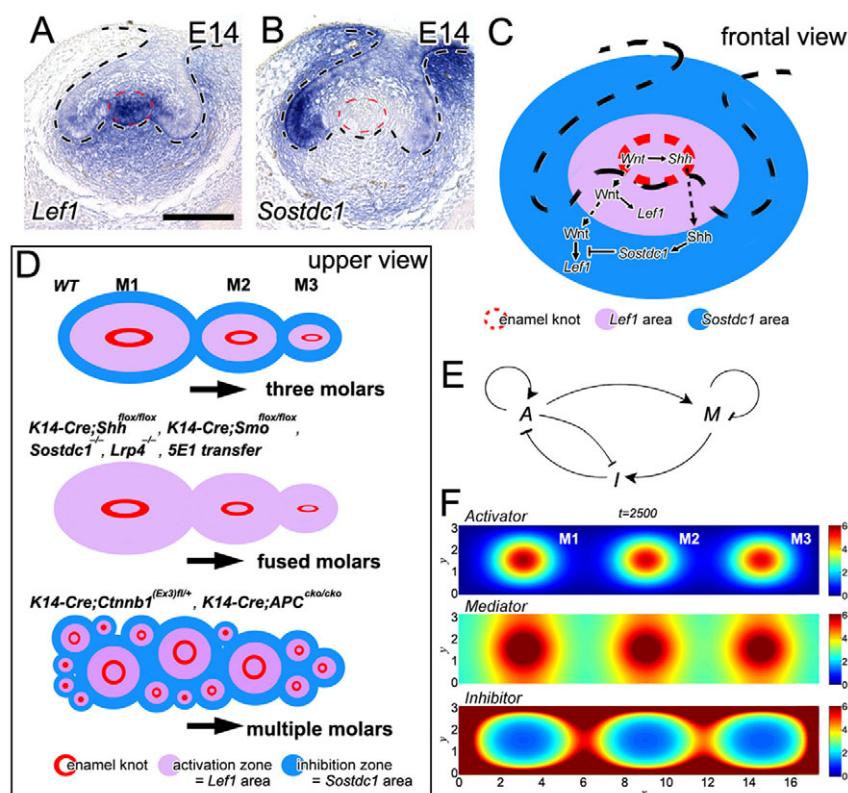


Fig. 6. Wnt-Shh-Sostdc1 negative feedback loop for the regulation of the tooth spatial patterning. (A, B) Frontal section of M1 at E14 shows that *Lef1* is expressed in the enamel knot (inside the red dashed circles) and dental mesenchyme surrounding the enamel knot, whereas *Sostdc1* is expressed mainly outside the *Lef1*-expressing area. (C) Schematic of Wnt-Shh-Sostdc1 negative feedback loop in M1 at E14 from frontal view. Wnt signals in the enamel knot induce *Shh* in the enamel knot and Wnt moves laterally to induce *Lef1* and *Sp5*. Secreted *Shh* in the enamel knot also moves laterally to induce *Sostdc1*. The *Sostdc1*-expressing area (*Sostdc1* area) is non-overlapping with the *Lef1*-expressing area (*Lef1* area). (D) Wild-type mouse has three molars, each of which has an activation zone (*Lef1* area) and an inhibition zone (*Sostdc1* area). Loss of the inhibition zone in *K14-Cre;Shh^{flox/flox}*, *K14-Cre;Smo^{flox/flox}*, *Sostdc1^{-/-}*, *Lrp4^{-/-}* and 5E1-transferred mice enhances molar fusion. Sustained Wnt/ β -catenin signals in *K14-Cre;Ctnnb1^{(Ex3)^{fl/+}}* and *K14-Cre;APC^{cko/cko}* induce multiple activation and inhibition zones to form multiple molars. (E) Schematic of the proposed reaction-diffusion model showing interactions between activator (A), mediator (M) and inhibitor (I). (F) Simulated patterns of activator, mediator and inhibitor show three molars in wild-type mice. The black dotted lines in A-C indicate the boundary of the dental epithelium and mesenchyme. Scale bar: 100 μm .

(Dassule et al., 2000; Gritli-Linde et al., 2002) suggests that an early effect of lack of Shh signaling is failure of formation of the dental lamina.

Sostdc1 is a target of Shh signaling in tooth development

M1-M2 fusions, like those seen in *K14-Cre;Shh^{flox/flox}* and *K14-Cre;Smo^{flox/flox}* transgenic mice and produced in our study by injecting 5E1, have also been observed in *Sostdc1^{-/-}* and *Lrp4^{-/-}* mice, as have supernumerary molars and incisors (Kassai et al., 2005; Ohazama et al., 2008). We found that *Sostdc1* expression was downregulated both in microarray and in RT-qPCR analyses and that there was no detectable expression of *Sostdc1* expression in dental mesenchyme from mice treated with the Shh blocking antibody at E14. Furthermore, we showed that *Sostdc1* expression can be induced in the dental mesenchyme at E14 by exogenous Shh protein. All these data are consistent with mesenchymal *Sostdc1* expression being a downstream target of Shh signaling. Furthermore there is another recent report that *Sostdc1* is one of the targets of Ihh signaling that is independent of Gli1 (Guo et al., 2010). However, in previously published work on tooth germs (Laurikkala et al., 2003), it was reported that *Sostdc1* expression was not induced in the mesenchyme when exogenous Shh protein was applied to intact germs without separation of dental epithelium and mesenchyme. We have confirmed this result. One of the possible reasons for the different response of the mesenchyme of intact tooth germs compared with dental mesenchyme on its own is that induction of mesenchymal *Sostdc1* expression by Shh might be inhibited by some endogenous factor in the intact tooth germ.

It was striking that *Sostdc1* was not induced in dental epithelium by applying Shh protein. If one takes *Ptch1* expression as an indication that cells have received an Shh signal, then endogenous expression of *Ptch1* in both the PBS- and Shh-treated dental

epithelium of wild-type mice suggests that both tissues had received the Shh signal. Furthermore, in the same series of experiments, exogenous Shh can induce *Ptch1* expression in dental epithelium. Finally, although blockade of Shh activity by 5E1 abolished *Ptch1* expression, *Sostdc1* was still expressed in dental epithelium. These results suggest that epithelial *Sostdc1* is not regulated by Shh and, indeed, it has been reported that epithelial *Sostdc1* can be induced by Bmp4 protein (Kassai et al., 2005).

Sostdc1 and Wnt signaling in spatial patterning of teeth

Sostdc1 is known to be a secreted inhibitor of the Wnt and Bmp pathways (Laurikkala et al., 2003; Yanagita et al., 2004; Ohazama et al., 2008; Munne et al., 2009) and recently, by utilizing Wnt reporter mice, elevated Wnt signaling was reported in *Sostdc1^{-/-}* mice, and reduced Wnt signaling was reported in *K14-Sostdc1* mice, which show ectopic expression of *Sostdc1* in epithelium (Ahn et al., 2010). In our study, decreased expression of *Sostdc1*, following the blocking of Shh activity by 5E1, would be predicted to lead to increase of Wnt/ β -catenin signaling. However, expression levels and patterns of β -catenin and *Lef1* were not changed by 5E1 treatment. This result is consistent with previous findings that *Lef1* expression levels showed minor alterations in *Sostdc1^{-/-}* mice, compared with *Sostdc1^{+/-}* mice, even though Wnt signaling activity was elevated (Ahn et al., 2010). However, we found that expression levels of *Sp5* were increased in microarray and RT-qPCR analyses and ectopic *Sp5* expression was also observed. As *Sp5*, which is expressed only in dental epithelium, at least from E12 to E16, is a direct transcriptional target of the Wnt/ β -catenin pathway, and the promoter region of *Sp5* contains multiple binding sites for *Lef1* and *Tcf* family members (Weidinger et al., 2005; Zhang et al., 2008), *Sp5* can be regarded as a good marker for Wnt/ β -catenin activity in dental epithelium. Therefore, we suggest that this upregulation

of *Sp5* indicates increased Wnt/ β -catenin signaling following blockade of Shh activity by 5E1. In addition, we found that *Sp5*-expressing areas in M1 and M2 were connected after blocking of Shh activity by 5E1 treatment, which might be the cause of the M1-M2 fusion.

A Wnt-Shh-Sostdc1 negative feedback loop in tooth patterning

In tooth development, it has been reported that Wnt/ β -catenin signals are upstream of Shh (Kratochwil et al., 2002; Jarvinen et al., 2006; Liu et al., 2008; Närhi et al., 2008) and Sostdc1 (Jarvinen et al., 2006; Närhi et al., 2008; Liu et al., 2008). By contrast, it was also reported that Shh suppresses Wnt/ β -catenin signaling in early developing mandible (Dassule and McMahon, 1998). Furthermore, a Wnt-Shh negative feedback loop in tooth development was recently suggested by the significant elevation of Wnt signaling in *Sostdc1*^{+/-};*Shh*^{+/-} mice, compared with that in *Sostdc1*^{+/-} mice (Ahn et al., 2010). In our study, the induction of *Sostdc1* by Shh protein in dental mesenchyme and the elevation of Wnt/ β -catenin signaling after blocking Shh signaling activity suggest a Wnt-Shh-Sostdc1 negative feedback loop, in which Wnt signaling induces Shh and Shh suppresses the Wnt/ β -catenin pathway indirectly via Sostdc1, as a candidate mechanism for tooth patterning.

Fgf4 and *Fgf3* have been reported as downstream genes of Wnt/ β -catenin pathway (Chamorro et al., 2005; Hendrix et al., 2006; Kratochwil et al., 2002), and the Fgf pathway was suggested as one of major downstream targets of Wnt signaling regulated by Sostdc1 (Ahn et al., 2010). Therefore, the overactivation of Wnt/ β -catenin signaling via downregulation of *Sostdc1* after 5E1 injection might be the cause of the increase of Fgf gene expression. In our study, mesenchymal Fgf genes, such as *Fgf3* and *Fgf10*, did not display any significant change in gene expression levels, whereas epithelial Fgf genes, such as *Fgf4*, *Fgf9* and *Fgf20*, exhibited significant changes following 5E1 treatment, which might be attributable to the elevation of *Sp5* expression in enamel knot.

Another pathway regulated by Sostdc1 downstream of Wnt signaling appears to be the Shh pathway itself. *Shh* expression was also found to be elevated in *Sostdc1*^{+/-} mice (Ahn et al., 2010) and in our study we found 1.4-fold increases in *Shh* expression after 5E1 treatment and premature *Shh* expression in M2 development. An increase in *Shh* expression would be consistent with a Wnt-Shh-Sostdc1 negative feedback loop.

Sostdc1 is a Bmp antagonist as well as an antagonist of the Wnt/ β -catenin pathway. Recent work comparing tooth germs of E13.5 *Sostdc1*^{+/-} mice with those of *Sostdc1*^{+/-} mice, showed major changes in components of the Wnt, Fgf and Shh pathways but minor alterations in Bmp and/or Tgf β or other pathways (Ahn et al., 2010). In addition, our results showing minor changes in expression levels in the Bmp pathway after 5E1 treatment highlight the role of Sostdc1 as a Wnt antagonist in tooth development. Nevertheless, Sostdc1 might have a close relationship with Bmp signals in teeth. For example, the development of extra molars and incisors in *Sostdc1*^{+/-} mice was accelerated by exogenous Bmp4 protein compared with wild-type mice (Kassai et al., 2005; Munne et al., 2009). However, the role of Bmp signals in the spatial patterning of teeth still remains to be elucidated, because conditional Bmpr1a-deficient mice such as *K14-Cre43;Bmpr1a*^{lox/flox} exhibit failure of tooth development after the bud stage (Andl et al., 2004), and *Sostdc1*^{+/-};*Bmpr1a*^{+/-} mice, in which levels of Bmp signaling were reduced through removal of a copy of the Bmpr1a type I receptor gene, do not show tooth phenotypes different from those of *Sostdc1*^{+/-} mice (Ahn et al., 2010).

Our results show that injection of an antibody against a specific signaling molecule into pregnant mice at chosen time points can be used to explore the relationships between signaling pathways in developing organs at various embryonic stages. By utilizing this method, we found evidence to suggest a Wnt-Shh-Sostdc1 negative feedback loop governing the spatial patterning of teeth. The loop described here might be a general reaction-diffusion mechanism for achieving the spatial pattern of other organs in vertebrates from fish to human. In our new model for spatial patterning of the teeth, Wnt, Shh and Sostdc1 act as activator, mediator and inhibitor, respectively (Fig. 6E). In this 'proof of concept' model of the spatial patterning of teeth, we have simply chosen the boundary conditions and form of growth to allow the system to recapitulate experimental observations. We need the Dirichlet (fixed) boundary conditions to stop pattern forming on the sides of the domain and we need the Neumann (zero flux) boundary conditions to stop diffusion of the mediator out of the domain. These boundary conditions are possible from a biological viewpoint, as they represent sinks and impermeability, respectively. They should be seen as predictions of the model. Our model is in contrast with a recent Salazar-Ciudad and Jernvall model (Salazar-Ciudad and Jernvall, 2010), which suggests that both Shh and Sostdc1 act as inhibitors. These two models are complementary in that we are trying to understand position, whereas they are trying to understand shape.

Acknowledgements

This research was supported by the Basic Science Research Program through the National Research Foundation of Korea (NRF) funded by the Ministry of Education, Science and Technology (R13-2003-013-05001-0). T.E.W. thanks the EPSRC for a studentship in Mathematics. R.E.B. thanks Research Councils UK for an RCUK Fellowship in Mathematical Biology and St Hugh's College, Oxford for a Junior Research Fellowship. P.K.M. was partially funded by a Royal Society Wolfson Research Merit Award. C.T. was funded by The Royal Society. We also thank G. H. Park, J. O. Shin, H. J. Kwon, J. M. Lee and K. W. Cho for help with in situ hybridization; W. C. Song for help with three-dimensional reconstructions; and K. S. Hu for comments.

Competing interests statement

The authors declare no competing financial interests.

Supplementary material

Supplementary material for this article is available at <http://dev.biologists.org/lookup/suppl/doi:10.1242/dev.056051/-DC1>

References

- Ahn, Y., Sanderson, B. W., Klein, O. D. and Krumlauf, R. (2010). Inhibition of Wnt signaling by Wise (Sostdc1) and negative feedback from Shh controls tooth number and patterning. *Development* **137**, 3221-3231.
- Andl, T., Ahn, K., Kairo, A., Chu, E. Y., Wine-Lee, L., Reddy, S. T., Croft, N. J., Cebra-Thomas, J. A., Metzger, D., Chambon, P. et al. (2004). Epithelial Bmpr1a regulates differentiation and proliferation in postnatal hair follicles and is essential for tooth development. *Development* **131**, 2257-2268.
- Cai, J., Cho, S. W., Kim, J. Y., Lee, M. J., Cha, Y. G. and Jung, H. S. (2007). Patterning the size and number of tooth and its cusps. *Dev. Biol.* **304**, 499-507.
- Chamorro, M. N., Schwartz, D. R., Vonica, A., Brivanlou, A. H., Cho, K. R. and Varmus, H. E. (2005). FGF-20 and DKK1 are transcriptional targets of beta-catenin and FGF-20 is implicated in cancer and development. *EMBO J.* **24**, 73-84.
- Crampin, E. J., Hackborn, W. W. and Maini, P. K. (2002). Pattern formation in reaction-diffusion models with nonuniform domain growth. *Bull. Math. Biol.* **64**, 747-769.
- Cui, C. Y., Hashimoto, T., Grivennikov, S. I., Piao, Y., Nedospasov, S. A. and Schlessinger, D. (2006). Ectodysplasin regulates the lymphotoxin-beta pathway for hair differentiation. *Proc. Natl. Acad. Sci. USA* **103**, 9142-9147.
- Dassule, H. R. and McMahon, A. P. (1998). Analysis of epithelial-mesenchymal interactions in the initial morphogenesis of the mammalian tooth. *Dev. Biol.* **202**, 215-227.
- Dassule, H. R., Lewis, P., Bei, M., Maas, R. and McMahon, A. P. (2000). Sonic hedgehog regulates growth and morphogenesis of the tooth. *Development* **127**, 4775-4785.
- Gaide, O. and Schneider, P. (2003). Permanent correction of an inherited ectodermal dysplasia with recombinant EDA. *Nat. Med.* **9**, 614-618.

- Gierer, A. and Meinhardt, H. (1972). A theory of biological pattern formation. *Kybernetik* **12**, 30-39.
- Gritli-Linde, A., Lewis, P., McMahon, A. P. and Linde, A. (2001). The whereabouts of a morphogen: direct evidence for short- and graded long-range activity of hedgehog signaling peptides. *Dev. Biol.* **236**, 364-386.
- Gritli-Linde, A., Bei, M., Maas, R., Zhang, X. M., Linde, A. and McMahon, A. P. (2002). Shh signaling within the dental epithelium is necessary for cell proliferation, growth and polarization. *Development* **129**, 5323-5337.
- Guo, S., Zhou, J., Gao, B., Hu, J., Wang, H., Meng, J., Zhao, X., Ma, G., Lin, C., Xiao, Y. et al. (2010). Missense mutations in IHH impair Indian Hedgehog signaling in C3H10T1/2 cells: Implications for brachydactyly type A1, and new targets for Hedgehog signaling. *Cell Mol. Biol. Lett.* **15**, 153-176.
- Hendrix, N. D., Wu, R., Kuick, R., Schwartz, D. R., Fearon, E. R. and Cho, K. R. (2006). Fibroblast growth factor 9 has oncogenic activity and is a downstream target of Wnt signaling in ovarian endometrioid adenocarcinomas. *Cancer Res.* **66**, 1354-1362.
- Iwatsuki, K., Liu, H. X., Grönder, A., Singer, M. A., Lane, T. F., Grosschedl, R., Mistretta, C. M. and Margolske, R. F. (2007). Wnt signaling interacts with Shh to regulate taste papilla development. *Proc. Natl. Acad. Sci. USA* **104**, 2253-2258.
- Järvinen, E., Salazar-Ciudad, I., Birchmeier, W., Taketo, M. M., Jernvall, J. and Thesleff, I. (2006). Continuous tooth generation in mouse is induced by activated epithelial Wnt/beta-catenin signaling. *Proc. Natl. Acad. Sci. USA* **103**, 18627-18632.
- Jernvall, J. and Thesleff, I. (2000). Reiterative signaling and patterning during mammalian tooth morphogenesis. *Mech. Dev.* **92**, 19-29.
- Johnson, E. B., Hammer, R. E. and Herz, J. (2005). Abnormal development of the apical ectodermal ridge and polysyndactyly in *Megf7*-deficient mice. *Hum. Mol. Genet.* **14**, 3523-3538.
- Kassai, Y., Munne, P., Hotta, Y., Penttilä, E., Kavanagh, K., Ohbayashi, N., Takada, S., Thesleff, I., Jernvall, J. and Itoh, N. (2005). Regulation of mammalian tooth cusp patterning by ectodin. *Science* **309**, 2067-2070.
- Kavanagh, K. D., Evans, A. R. and Jernvall, J. (2007). Predicting evolutionary patterns of mammalian teeth from development. *Nature* **449**, 427-432.
- Khaejornbut, J., Wilson, D. J. and Owens, P. D. A. (1991). The development and fate of the dental lamina of the mandibular first molar tooth in the rat. *J. Anat.* **179**, 85-96.
- Kratochwil, K., Galceran, J., Tontsch, S., Roth, W. and Grosschedl, R. (2002). FGF4, a direct target of LEF1 and Wnt signaling, can rescue the arrest of tooth organogenesis in *Left1*^{-/-} mice. *Genes Dev.* **16**, 3173-3185.
- Kuraguchi, M., Wang, X. P., Bronson, R. T., Rothenberg, R., Ohene-Baah, N. Y., Lund, J. J., Kucherlapati, M., Maas, R. L. and Kucherlapati, R. (2006). Adenomatous polyposis coli (APC) is required for normal development of skin and thymus. *PLoS Genet.* **2**, e146.
- Laurikkala, J., Kassai, Y., Pakkasjarvi, L., Thesleff, I. and Itoh, N. (2003). Identification of a secreted BMP antagonist, ectodin, integrating BMP, FGF, and SHH signals from the tooth enamel knot. *Dev. Biol.* **264**, 91-105.
- Lipinski, R. J., Hutson, P. R., Hannam, P. W., Nydza, R. J., Washington, I. M., Moore, R. W., Girdaukas, G. G., Peterson, R. E. and Bushman, W. (2008). Dose- and route-dependent teratogenicity, toxicity, and pharmacokinetic profiles of the hedgehog signaling antagonist cyclopamine in the mouse. *Toxicol. Sci.* **104**, 189-197.
- Liu, F., Chu, E. Y., Watt, B., Zhang, Y., Gallant, N. M., Andl, T., Yang, S. H., Lu, M. M., Piccolo, S., Schmidt-Ullrich, R. et al. (2008). Wnt/beta-catenin signaling directs multiple stages of tooth morphogenesis. *Dev. Biol.* **313**, 210-224.
- Munne, P. M., Tummers, M., Järvinen, E., Thesleff, I. and Jernvall, J. (2009). Tinkering with the inductive mesenchyme: *Sostdc1* uncovers the role of dental mesenchyme in limiting tooth induction. *Development* **136**, 393-402.
- Närhi, K., Järvinen, E., Birchmeier, W., Taketo, M., Mikkola, M. and Thesleff, I. (2008). Sustained epithelial β -catenin activity induces precocious hair development but disrupts hair follicle down-growth and hair shaft formation. *Development* **135**, 1019-1028.
- Ohazama, A., Johnson, E. B., Ota, M. S., Choi, H. Y., Porntaveetus, T., Ommen, S., Itoh, N., Eto, K., Gritli-Linde, A., Herz, J. et al. (2008). *Lrp4* modulates extracellular integration of cell signaling pathways in development. *PLoS One* **3**, e4092.
- Salazar-Ciudad, I. and Jernvall, J. (2002). A gene network model accounting for development and evolution of mammalian teeth. *Proc. Natl. Acad. Sci. USA* **99**, 8116-8120.
- Salazar-Ciudad, I. and Jernvall, J. (2010). A computational model of teeth and the developmental origins of morphological variation. *Nature* **464**, 583-586.
- St-Jacques, B., Dassule, H. R., Karavanova, I., Botchkarev, V. A., Li, J., Danielian, P. S., McMahon, J. A., Lewis, P. M., Paus, R. and McMahon, A. P. (1998). Sonic hedgehog signaling is essential for hair development. *Curr. Biol.* **8**, 1058-1068.
- Thesleff, I. (2003). Epithelial-mesenchymal signaling regulating tooth morphogenesis. *J. Cell Sci.* **116**, 1647-1648.
- Turing, A. (1952). The chemical basis of morphogenesis. *Philos. Trans. R. Soc. Lond. B Biol. Sci.* **237**, 37-72.
- Wang, B., Fallon, J. F. and Beachy, P. A. (2000). Hedgehog-regulated processing of *Gli3* produces an anterior/posterior repressor gradient in the developing vertebrate limb. *Cell* **100**, 423-434.
- Wang, L. C., Liu, Z. Y., Gambardella, L., Delacour, A., Shapiro, R., Yang, J., Sizing, I., Rayhorn, P., Garber, E. A., Benjamin, C. D. et al. (2000). Regular articles: conditional disruption of hedgehog signaling pathway defines its critical role in hair development and regeneration. *J. Invest. Dermatol.* **114**, 901-908.
- Weidinger, G., Thorpe, C. J., Wuennenberg-Stapleton, K., Ngai, J. and Moon, R. T. (2005). The Sp1-related transcription factors *sp5* and *sp5-like* act downstream of Wnt/beta-catenin signaling in mesoderm and neuroectoderm patterning. *Curr. Biol.* **15**, 489-500.
- Yanagita, M., Oka, M., Watabe, T., Iguchi, H., Niida, A., Takahashi, S., Akiyama, T., Miyazono, K., Yanagisawa, M. and Sakurai, T. (2004). USAG-1: a bone morphogenetic protein antagonist abundantly expressed in the kidney. *Biochem. Biophys. Res. Commun.* **316**, 490-500.
- Zhang, Y., Andl, T., Yang, S. H., Teta, M., Liu, F., Seykora, J. T., Tobias, J. W., Piccolo, S., Schmidt-Ullrich, R., Nagy, A. et al. (2008). Activation of beta-catenin signaling programs embryonic epidermis to hair follicle fate. *Development* **135**, 2161-2172.